The Crucial Role of Cyclooxygenase-2 in Osteopontin-Induced Protein Kinase C α/c-Src/IκB Kinase α/β–Dependent Prostate Tumor Progression and Angiogenesis

Shalini Jain, Goutam Chakraborty, and Gopal C. Kundu

National Center for Cell Science, Pune, India

Abstract

The regulation of tumor progression towards its malignancy needs the interplay among several cytokines, growth factors, and enzymes, which are controlled in the tumor microenvironment. Here, we report that osteopontin, a small integrin-binding ligand N-linked glycoprotein family of calcified extracellular matrix–associated protein, regulates prostate tumor growth by regulating the expression of cyclooxygenase-2 (COX-2). We have shown that osteopontin stimulates the activation of protein kinase C α/nuclear factor–inducing kinase/nuclear factor-κB–dependent signaling cascades that induces COX-2 expression, which in turn regulates the prostaglandin E_2 production, matrix metalloproteinase-2 activation, and tumor progression and angiogenesis. We have revealed that suppression of osteopontin-induced COX-2 expression by the nonsteroidal anti-inflammatory drug celecoxib or blocking the EP2 receptor by its blocking antibody resulted in significant inhibition of cell motility and tumor growth and angiogenesis. The data also showed that osteopontin-induced mice PC-3 xenograft exhibits higher tumor load, increased tumor cell infiltration, nuclear polymorphism, and neovascularization. Interestingly, use of celecoxib or anti-EP2 blocking antibody drastically suppressed osteopontin-induced tumor growth that further indicated that suppression of COX-2 or its metabolites could significantly inhibit osteopontin-induced tumor growth. Human clinical prostate cancer specimen analysis also supports our *in vitro* and animal model studies. Our findings suggest that blockage of osteopontin and/or COX-2 is a promising therapeutic approach for the inhibition of prostate tumor progression and angiogenesis. (Cancer Res 2006; 66(13): 6638-48)

Introduction

Cancer of the prostate is the most frequently diagnosed cancer and one of the major causes of death in men especially in western world (1). Prostate cancer progression is a series of complex events, which require crosstalk between several oncogenic molecules, and enable the cancer to spread and evoke angiogenesis. A high level of constitutive cyclooxygenase-2 (COX-2) expression has been detected in colorectal, gastric, pancreatic, head and neck, lung, breast, and in other cancers (2). COX is an integral membrane bifunctional enzyme, which metabolizes arachidonic acids to many biologically active eicosanoids (3–5). There are three isoforms of the COX enzyme (COX-1, COX-2, and COX-3). COX-1 is involved in the production of prostaglandin (PG)–mediating cellular and physiologic functions. The functional role of COX-3 in human physiology and pathophysiology remains to be established (6).

COX-2 is induced in many cell types by mitogens, growth factors, cytokines, and tumor promoters, and its increased expression is associated with cancer progression through a PG-dependent manner (2–5). COXs convert free arachidonic acids into PGs and thromboxanes (3). In human prostate carcinoma, significant levels of PGE_2 has been detected, which plays an important role in cancer progression (7). PGE_2 can contribute to tumor development through several mechanisms, including promotion of angiogenesis, inhibition of apoptosis, increased invasiveness and motility, and modulation of inflammation and immune responses (8–10). Recent reports showed that COX-2 promotes tumor cell proliferation, survival, and angiogenesis through a PGE_2-mediated pathway (10, 11).

Osteopontin, a secreted, noncollagenous, chemokine-like small integrin-binding ligand N-linked glycoprotein family of protein plays significant role in determining the oncogenic potential of various cancers and recognized as a key marker in the processes of tumorigenicity and metastasis (12). Osteopontin is an acidic glycoprotein with a molecular mass varying from 44 to 75 kDa, depending on the degree of posttranslational modification (13). It has an NH_2-terminal signal sequence, a sialic acid region consisting of nine consecutive aspartic acid residues, a GRGDS cell adhesion sequence that is predicted to be flanked by β-sheet structure (14). Osteopontin interacts with several integrins and CD44 variants in an RGD sequence–dependent and RGD sequence–independent manner (15, 16). Osteopontin is involved in normal tissue remodeling processes, such as bone resorption, wound healing, and tissue injuries as well as restenosis, atherosclerosis, tumorigenesis, and autoimmune diseases (17, 18). Previous studies indicated that osteopontin plays crucial role in chemotaxis and chemoinvasion of PC-3 cells (19). Recent data also showed that osteopontin induces pro-matrix metalloproteinase-2 (pro-MMP-2) and pro-MMP-9 activation, urokinase plasminogen activator (uPA) secretion, cell motility, extracellular matrix invasion, and tumor growth (20, 21).

Cell motility, a major step in cancer metastasis, is often associated with the activation of protein tyrosine or serine kinases, like c-Src and protein kinase C α (PKCα), respectively. Previous studies have indicated that c-Src and PKCα play crucial roles in COX-2 expression and COX-2-dependent tumor progression (22–24). The transcription factor nuclear factor-κB (NF-κB) act as a key molecule in regulating wide range of physiologic and pathologic processes (25). Nuclear factor inducing kinase (NIK), a member of mitogen-activated protein kinase kinase kinase (MAPKKK) family has been reported to activate NF-κB through phosphorylation and degradation of IκBα (26). We have recently

Requests for reprints: Gopal C. Kundu, National Center for Cell Science, Pune 411 007, India. Phone: 91-20-25690922 ext. 1103; Fax: 91-20-25692259; E-mail: kundu@nccs.res.in.

doi:10.1158/0008-5472.CAN-06-0661

reported that osteopontin induces uPA secretion and MMP-2/MMP-9 activation through c-Src/phosphatidylinositol 3-kinase/MAPK signaling pathways (20, 21, 27). However, the molecular mechanism by which osteopontin regulates PKCα/c-Src–dependent IκB kinase (IKK)–mediated NF-κB activation, which ultimately regulates tumor progression and angiogenesis through induction of COX-2 expression in prostate cancer and signaling cascades, underlying these processes are not well defined.

In this study, we provide both *in vitro* and *in vivo* experimental evidences, at least in part, the molecular mechanism by which osteopontin regulates PKCα/c-Src/IKK/NF-κB signaling cascades leading to COX-2-mediated PGE_2 production and MMP-2 activation in prostate cancer. Furthermore, we have shown that osteopontin-induced COX-2 regulates cell motility, angiogenesis, and tumorigenesis of prostate cancer through both autocrine and paracrine pathways. However, suppression of COX-2 activity by nonsteroidal anti-inflammatory drug (NSAID) celecoxib or blocking the interaction between PGE_2 and its receptor EP2 by using specific anti-EP2 blocking antibody significantly suppressed osteopontin-induced *in vitro* cell motility, invasiveness, and *in vivo* tumor growth. Moreover, the clinical data indicated that the increased expressions of osteopontin and COX-2 correlate with enhanced MMP-2 expression and angiogenesis in prostate cancer specimens of higher grades. Consequently, osteopontin plays important and essential role in two key aspects of tumor progression: COX-2-mediated PGE_2 production and MMP-2 activation by tumor cells leading to tumor progression and COX-2/PGE_2–stimulated angiogenesis. Our findings suggest that blockade of osteopontin and COX-2 is a promising therapeutic approach for the inhibition of tumor progression by suppressing tumor growth and angiogenesis.

Materials and Methods

Antibodies and reagents. Rabbit polyclonal anti-COX-2, anti-PKCα, anti-NIK, anti-p-NIK(Thr^{559}), anti-IKKα/β, anti-NF-κB, p65, anti-MMP-2, anti-c-Src, anti-EP2, and anti-actin, mouse monoclonal anti-phosphotyrosine, goat polyclonal anti-phospho-PKCα (Ser^{657}) antibodies were purchased from Santa Cruz Biotechnology (Santa Cruz, CA). Rabbit polyclonal anti-p-IKKα/β (Ser^{180}/Ser^{181}) antibody was from Cell Signaling Technology (Beverly, MA); goat polyclonal anti-osteopontin antibody was from R&D Systems (Minneapolis, MN); and rabbit polyclonal anti-human vWF antibody was purchased from Sigma (St. Louis, MO). The [γ-^{32}P]ATP was purchased from Board of Radiation and Isotope Technology (Hyderabad, India). All other chemicals were of analytic grade. The human osteopontin was purified from milk as described previously (20), with a minor modification, and used throughout this study.

Cell culture. The human prostate cancer (PC-3) cells were obtained from the American Type Culture Collection (Manassas, VA). Human umbilical vein endothelial cell line EA.hy-926 was a generous gift from Dr. Christopher Newton (University of Hull, United Kingdom). PC-3 cells were cultured in F-12 HAM Nutrient Mixture (Sigma), and EA.hy-926 cells were cultured in DMEM (Sigma) supplemented with 10% FCS, 100 units/mL penicillin, 100 μg/mL streptomycin, and 2 mmol/L glutamine in a humidified atmosphere of 5% CO_2 and 95% air at 37°C.

Plasmids and DNA transfection. The full-length osteopontin cDNA was a generous gift from Dr. Ann Chambers (University of Western Ontario, London, Ontario, Canada). The dominant-negative c-Src (pcSrcY527F/S12A) and COX-2-Luc (−1432/+59) constructs were generous gifts from Dr. David Shalloway (Cornell University, NY) and Dr. Hiroyashu Inoue (Osaka, Japan; ref. 28), respectively. The wild-type NIK (wt pcDNA NIK) and kinase-negative NIK (mut pc DNA NIK and NIK-K429A/K430A) in pcDNA3 were obtained from Prof. David Wallach (Weizmann Institute of Science, Rehovot, Israel). The wild-type and dominant-negative constructs of IKKα (wt IKKα and dn IKKα) and IKKβ (wt IKKβ and dn IKKβ) in PKC-related kinase were kind gifts from Prof. D.V. Goeddel (Tularik, Inc., San Francisco, CA). The super-repressor form of IκBα cDNA fused downstream to a FLAG epitope in an expression vector (pCMV4) was a gift from Dr. Dean Ballard (Vanderbilt University School of Medicine, Nashville, TN). PC-3 cells were split 16 hours before transfection and transiently transfected with cDNA using LipofectAMINE 2000 reagent according to manufacturer's instructions (Invitrogen, San Diego, CA). The cell viability was detected by trypan blue dye exclusion test. Transfected cells were used for COX-2 expression, COX-2 promoter analysis studies, IKK and p65 phosphorylation, and PKCα kinase assay and migration and invasion assays.

Small interfering RNA. PC-3 cells were transfected with small interfering RNA (siRNA) that specifically targets the osteopontin gene or nonsilencing control using LipofectAMINE-2000 according to manufacturer's instructions. siRNA duplexes were synthesized by Dharmacon, Inc. (Lafayette, CO). The sequence targeted for osteopontin is 5′-GUUUCACAGCCACAAGGACdTdT/dTdTCAAAGUGUCGGUGUUCCUG-5′, and the nonsilencing control is 5′-CAGUACAACGCAUCUGGCAdTdT/dTdTGUCAUGUUGCGUAGACCGU-5′.

Western blot and immunoprecipitation. The level of COX-2, PKCα c-Src, osteopontin, IKKα/β, actin expressions and phosphorylations of IKKα/β and NF-κB, p65 in transfected or treated PC-3 cells were analyzed by Western blot using its specific antibody (20). The tyrosine phosphorylation of IKKα/β and the interaction between PKCα and c-Src were done by immunoprecipitation followed by Western blot.

RNA extraction and reverse transcription-PCR. Total RNA was isolated from osteopontin-treated PC-3 cells and analyzed by reverse transcription-PCR (RT-PCR). The reverse transcription and PCR amplification used 10 μg of total RNA, with Moloney murine leukemia virus reverse transcriptase (Invitrogen) and primers COX-2 forward (5′-TTCAAATGAGATTGTGGGAAAATTGCT-3′) and COX-2 reverse (5′-AGATCATCTCTGCCTGAGTATCTT-3′) to reverse transcribe sense and antisense RNAs, respectively (29). The amplified cDNA fragments were resolved by 2% agarose gel electrophoresis.

COX-2 luciferase assay. The semiconfluent PC-3 cells were grown in 24-well plates and transiently transfected with COX-2 luciferase reporter construct using LipofectAMINE 2000. In separate experiments, cells were individually transfected with wt and mut NIK and wt and dn IKKβ along with COX 2 luciferase construct. The transfection efficiency was normalized by cotransfecting the cells with pRL vector (Promega, Madison, WI) containing a full-length *Renilla* luciferase gene under the control of a constitutive promoter. After 24 hours of transfection, the cells were treated with 0.5 μmol/L osteopontin, and the luciferase activities were measured by luminometer (Thermo Electron) using the dual luciferase assay system according to the manufacturer's instructions (Promega). Changes in the luciferase activity with respect to control were calculated.

Estimation of PGE_2. The levels of PGE_2 from the conditioned media of osteopontin-treated PC-3 cells and mice plasma were detected by using the Biotrack PGE_2 competitive enzyme immunoassay kit (Amersham Biosciences, Piscataway, NJ) according to the manufacturer's instructions.

***In vitro* kinase assay by autophosphorylation study.** *In vitro* kinase assay was done as described earlier (30). Briefly, PC-3 cells were either treated with osteopontin (0.5 μmol/L) for 5 minutes or pretreated with 100 nmol/L staurosporine (Calbiochem, La Jolla, CA) for 3 hours or transfected with dn c-Src and then treated with osteopontin. Cell lysates were immunoprecipitated with anti-PKCα and anti-c-Src antibodies. Autophosphorylation of PKCα and c-Src were measured by incubating the immunoprecipitated samples with 40 μCi of [γ^{32}P]ATP in 40 μL kinase assay buffer [20 mmol/L HEPES (pH 7.7), 2 mmol/L $MgCl_2$, 10 mmol/L β-glycerophosphate, 10 mmol/L NaF, 10 mmol/L pNPP, 300 μmol/L Na_3VO_4, 1 mmol/L benzamidine, 2 μmol/L phenylmethylsulfonyl fluoride, 10 μg/mL aprotinin, 1 μg/mL leupeptin, 1 μg/mL pepstatin, and 1 mmol/L DTT] for 30 minutes at 30°C. Reactions were terminated by the addition of sample buffer and analyzed by SDS-PAGE followed by autoradiography.

Zymography. The gelatinolytic activity was measured as described previously (20). Briefly, PC-3 cells were either treated with osteopontin or pretreated with staurosporine and COX-2 inhibitor (Celecoxib) or

transfected with dn c-Src and then treated with osteopontin. Conditioned medium was collected, and gelatinolytic activity of MMP-2 was detected by zymography.

Cell migration and invasion assay. The migration and invasion assays were done using Transwell cell culture chamber (Corning, Corning, NY) and Matrigel coated invasion chambers (Collaborative Biomedical, Bedford, MA), respectively, according to the standard procedure as described previously (27). Briefly, the confluent monolayers of PC-3 (treated or transfected) cells were harvested with trypsin-EDTA and centrifuged at 800 $\times$ *g* for 10 minutes. The cell suspension (2×10^5 per well) was added to the upper chamber. The lower chamber was filled with fibroblast-conditioned medium, which acted as a chemoattractant. In separate experiments, osteopontin-treated conditioned medium of PC-3 cells was incubated with EA.hy-926 cells alone or along with anti-EP-2 blocking antibody and subjected to migration and invasion assays. After 12 hours, cells in the lower chamber were fixed and stained with Giemsa stain and counted in three high-power fields (C/HPF) under an inverted microscope (Olympus). Data are presented as the average of three counts $\pm$SE.

Wound assay. The wound assay was done as described (31). Briefly, the post-confluent PC-3 cells with typical cobblestone morphology were used in this experiment. Wounds with a constant diameter were made. Cells were treated with osteopontin alone or along with EP2 blocking antibody or celecoxib (COX-2 inhibitor). In other experiments, EA.hy-926 cells were incubated with conditioned media obtained from osteopontin-treated PC-3 cells either alone or along with EP2 blocking antibody, and wound assay was conducted. The wound photographs were taken under phase-contrast microscope (Olympus).

PC-3 xenograft tumor model. The tumorigenicity experiments were done as described previously (27). Briefly, PC-3 cells (5×10^5) were mixed with an equal volume of cold Matrigel and then injected s.c. into the dorsal side of the athymic nude mice (NMRI, *nu/nu*; NIV, Pune, India). Osteopontin alone or along with anti-EP-2 blocking antibody (20 μg) was injected into tumor sites twice a week for up to 4 weeks. In other experiments, celecoxib (1,500 ppm) was given along with diet of the osteopontin-injected animals as described earlier (32). Three mice were used in each set of experiments. The mice were kept under pathogen-free conditions. Growths of s.c. tumors were monitored weekly by measuring the tumors with calipers. At the termination of the experiment, blood was collected from the retro-orbital plexus under anesthesia from both experimental and control groups. Animals were sacrificed by cervical dislocation, and tumors were excised and weighed. The tumor samples were used for histopathologic and immunohistochemical studies using standard procedure (33). The expressions of COX-2, MMP-2, and vWF (endothelial cell–specific marker) were determined by immunofluorescence using their specific antibodies. The slides were analyzed under confocal microscopy (Zeiss, Jena, Germany).

Human prostate clinical sample analysis. Human prostate tumor specimens of different Gleason grades and normal prostate tissues were collected from a local hospital with informed consent. The COX-2, osteopontin, MMP-2, and vWF expressions were detected by immunofluorescence using specific antibodies. Five samples of each group [normal, low grade (prostatic intraepithelial neoplasia or PIN), and malignant] were analyzed. Normal prostate tissues were used as control.

Statistical analysis. The data reported in cell migration, wound healing, and invasion are expressed as mean $\pm$SE. Statistical differences were determined by two-way ANOVA and Student's *t* test. $P < 0.05$ was considered significant. All these bands were analyzed densitometrically (Kodak Digital Science, Rochester, NY), and the fold changes were calculated.

Results

Osteopontin augments COX-2 protein and mRNA expression. To determine whether osteopontin augments COX-2 expression, PC-3 cells were treated with 0.5 μmol/L osteopontin for 0 to 24 hours. Expression of COX-2 in cell lysates was detected by Western blot, and the data indicated that osteopontin

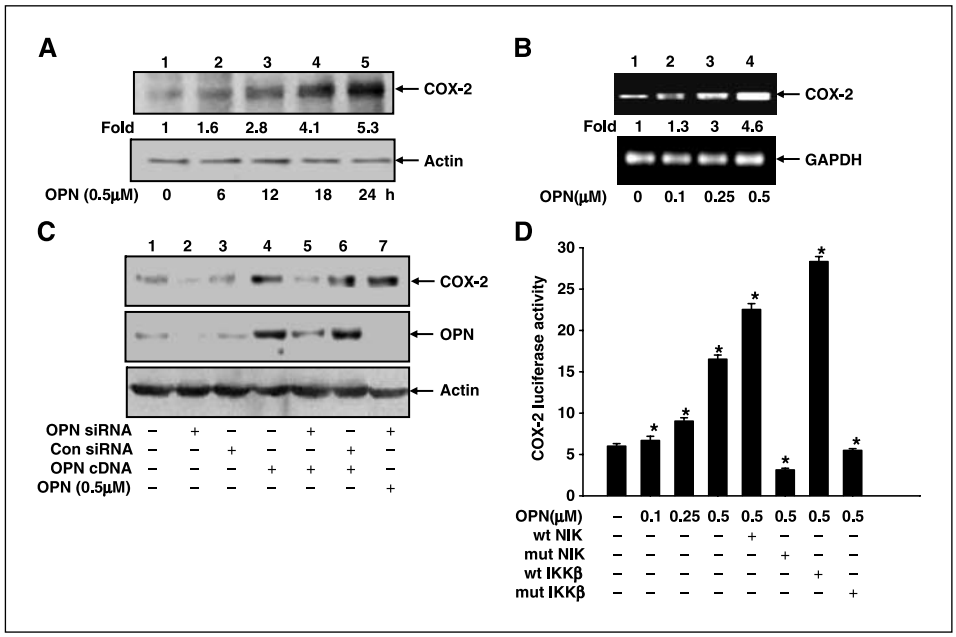

Figure 1. Osteopontin (*OPN*) induces COX-2 promoter activity and expression in PC-3 cells. *A,* serum-starved PC-3 cells were treated with 0.5 μmol/L osteopontin for 0 to 24 hours. The level of COX-2 from whole-cell lysates was analyzed by Western blot. Actin was used as loading control. *B,* cells were treated with osteopontin (0-0.5 μmol/L) for 6 hours; total RNA was isolated; and RT-PCR analysis was done using COX-2-specific primers. Changes in mRNA levels were determined as fold of induction. Glyceraldehyde-3-phosphate dehydrogenase (GAPDH) was used as internal control. *C,* PC-3 cells were transfected with osteopontin cDNA, osteopontin-specific siRNA, or nonsilencing scrambled siRNA. In separate experiments, osteopontin siRNA–transfected cells were either cotransfected with osteopontin cDNA or treated with 0.5 μmol/L osteopontin. COX-2 was analyzed by Western blot. The level of osteopontin is also detected by Western blot. Actin was used as loading control. *D,* osteopontin enhances NIK/IKK–mediated COX-2 promoter activity. Cells were transfected with luciferase reporter construct (COX-2-Luc) and then treated with 0 to 0.5 μmol/L osteopontin or cotransfected with wt and mut NIK or wt and dn IKKβ and then treated with 0.5 μmol/L osteopontin. Cell lysates were used to measure the luciferase activity. The values were normalized to *Renilla* luciferase activity. The fold changes were calculated. *Columns,* mean of triplicate determinations; *bars,* SE.

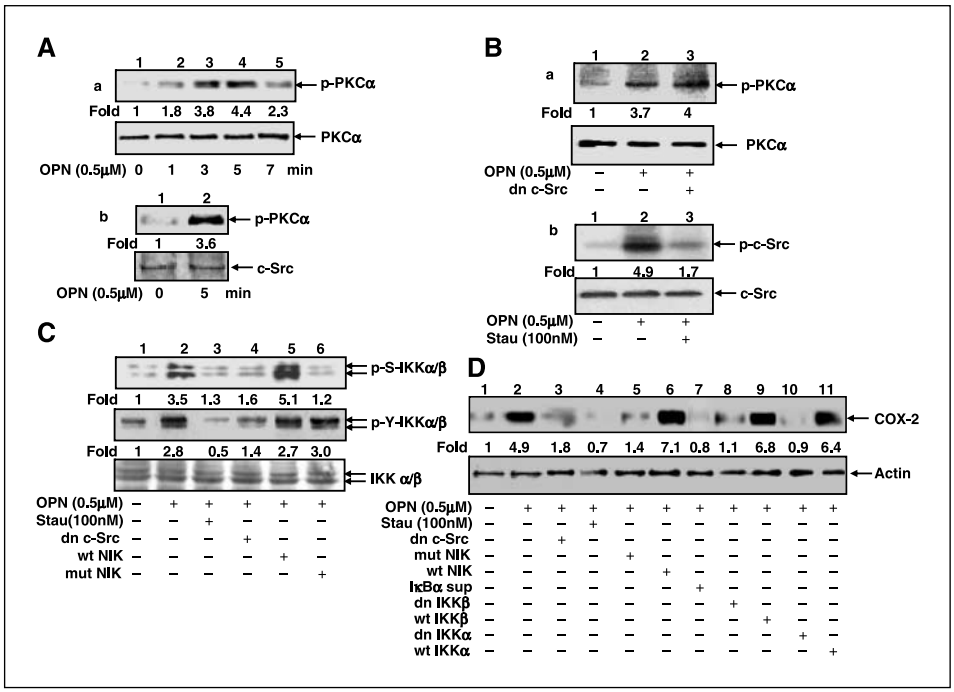

Figure 2. Osteopontin (*OPN*) induces PKCα activation, PKCα-mediated c-Src and IKK phosphorylation, and COX-2 expression. *A,* PC-3 cells were treated with osteopontin for 0 to 7 minutes, and the phosphorylation of PKCα was detected by Western blot using anti-phospho-PKCα antibody (*p-PKCα*; *a, top*). The cells were treated with osteopontin for 0 and 5 minutes, and cell lysates were immunoprecipitated with anti-c-Src antibody and analyzed by Western blot using anti-phospho-PKCα antibody (*b, top*). Levels of PKCα and c-Src were detected by reprobing the same blots with their specific antibodies (*a* and *b, bottom*). *B,* cells were either transfected with dn c-Src or pretreated with staurosporine (*Stau*, a PKC inhibitor, 100 nmol/L) and then treated with osteopontin for 5 minutes. Cell lyates were immunoprecipitated with anti-PKCα or anti-c-Src antibody, and the kinase activity of PKCα (*a*) and c-Src (*b*) was determined by autophosphorylation experiment and visualized by autoradiography. *C,* cells were individually transfected with dn c-Src, wt and mut NIK, or pretreated with staurosporine and then treated with osteopontin. Half of the cell lysates were analyzed by Western blot using anti-phospho-Ser-IKKα/β (Ser^{180}/Ser^{181}) antibody (*top*), and the remaining part of cell lysates was immunoprecipitated with IKKα/β antibody and detected by Western blot using anti-phosphotyrosine antibody (*middle*). The level of IKKα/β was also detected by Western blot (*bottom*). *D,* cells were pretreated with staurosporine or individually transfected with dn c-Src, IκBα super-repressor (*sup. rep.*), wt and dn IKKα or IKKβ, and wt or mut NIK and then treated with osteopontin. COX-2 expression was detected by Western blot. Actin was used as loading control. Represents three experiments exhibiting similar results. Fold changes were calculated.

induced maximum COX-2 expression at 24 hours (Fig. 1*A*). The dose-dependent effect of osteopontin (0-1 μmol/L) on COX-2 expression was also detected, and the results indicated that osteopontin at 0.5 μmol/L exhibits maximum level of COX-2 expression in PC-3 cells (data not shown). The COX-2 mRNA level was also determined by RT-PCR, and the data indicated that osteopontin at 0.5 μmol/L enhanced maximum COX-2 expression at transcriptional level (Fig. 1*B*). Interestingly, our results also showed that osteopontin induced COX-2 expression in other prostate cancer cell lines like DU-145 and LNCaP (data not shown). To examine the specificity of osteopontin on COX-2 expression, cells were transfected with wt osteopontin cDNA alone or cotransfected with osteopontin siRNA duplex and control RNA duplex. The data showed that cells transfected with osteopontin cDNA enhanced the COX-2 expression. Cells transfected with osteopontin cDNA followed by siRNA duplex suppressed the osteopontin-induced COX-2 expression (Fig. 1*C*). Our results indicated that osteopontin enhanced COX-2 expression both at transcriptional and translational levels.

Osteopontin enhances NIK/IKK/NF-κB–dependent COX-2 promoter activity. The effect of osteopontin on COX-2 promoter activity was determined by transfecting PC-3 cells with COX-2 luciferase construct followed by treatment with osteopontin in a dose-dependent manner. In separate experiments, cells were cotransfected with wt NIK or IKKβ or kinase-negative (mut) NIK or dn IKKβ along with COX-2 luciferase construct and then treated with osteopontin. Further transfecting the cells with pRL construct normalized the transfection efficiency, and COX-2 luciferase activities were measured according to standard procedure. The results showed that cells transfected with wt NIK or IKKβ enhanced the COX-2 promoter activity, whereas mut NIK or dn IKKβ significantly suppressed osteopontin-induced COX-2 promoter activity (Fig. 1*D*). Cells transfected with wt IKKα enhanced osteopontin-induced COX-2 promoter activity, whereas dn IKKα or the super-repressor form of IκBα suppressed osteopontin-induced COX-2 promoter activity (data not shown). These results indicated that osteopontin enhanced COX-2 promoter activity through a NIK/IKK–dependent NF-κB-mediated pathway.

Osteopontin regulates PKCα/c-Src–dependent IKK/NF-κB–mediated COX-2 expression. Recent reports revealed that PKCα plays important role in the survival and growth of androgen-independent human prostate cancer (PC-3) cells (34). It is well established that PKCα plays crucial role in COX-2 expression (23). Therefore, to delineate the effect of osteopontin on PKCα phosphorylation and its interaction with c-Src, cells were treated with osteopontin for 0 to 7 minutes, and one part of the cell lysates was analyzed by Western blot using anti-phospho-PKCα antibody (Fig. 2*A, a, top*). The remaining part of lysates was immunoprecipitated with anti-c-Src antibody, and the interaction between phosphorylated PKCα and c-Src was determined by Western blot using anti-phospho-PKCα antibody (Fig. 2*A, b, top*). The same blots were reprobed with anti-PKCα and c-Src antibody, respectively, as

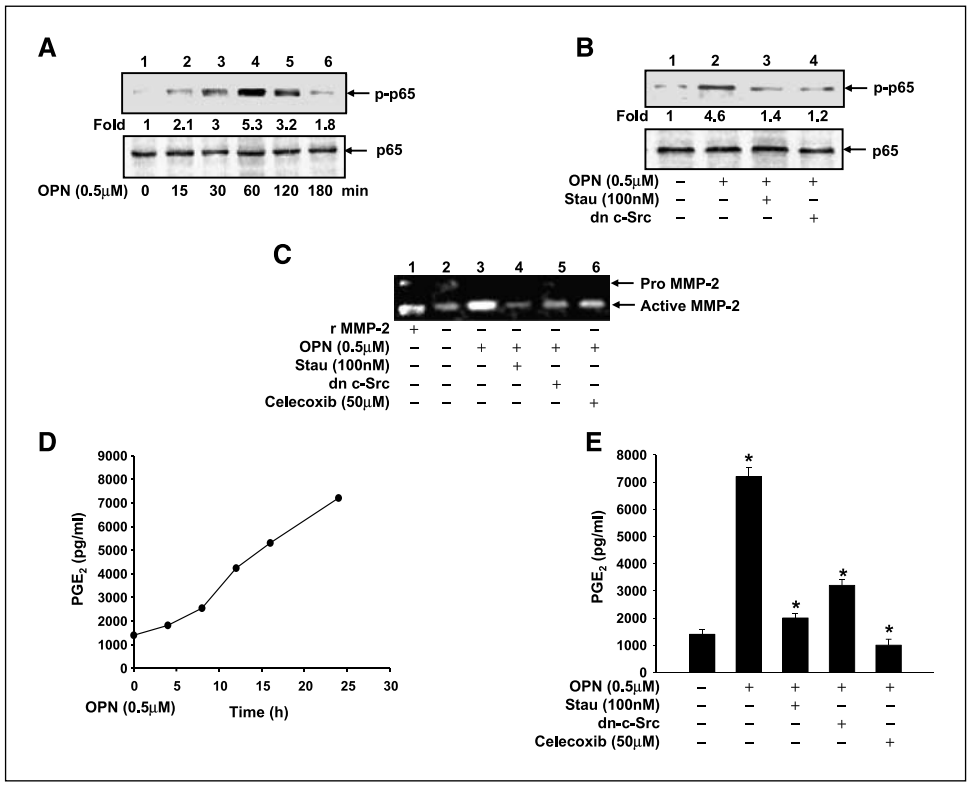

Figure 3. Osteopontin (*OPN*) induces PKCα/c-Src–dependent NF-κB, p65 phosphorylation, MMP-2 activation, and PGE_2 production. *A,* PC-3 cells were treated with osteopontin for the indicated time, and the level of phospho-p65 (*p-p65*; Ser^{536}) from cell lysates were detected by Western blot (*top*). *B,* cells were transfected with dn c-Src or pretreated with staurosporine (*Stau*) and then treated with osteopontin. The level of phospho-p65 was analyzed by Western blot. The level of non-phospho-p65 was also detected by Western blot (*A* and *B, bottom*). *C,* cells were transfected with dn c-Src or pretreated with staurosporine or celecoxib (COX-2 inhibitor, 50 μmol/L) and then treated with osteopontin for 24 hours. Conditioned media were collected, and the level of MMP-2 activation was detected by zymography. Recombinant MMP-2 (r MMP-2) was used as positive control. *D* and *E,* cells were treated with 0.5 μmol/L osteopontin for 0 to 24 hours. In separate experiments, cells were transfected with dn c-Src or pretreated with staurosporine and celecoxib and then treated with osteopontin for 24 hours. Conditioned media were collected, and the level of PGE_2 was estimated by enzyme immunoassay. Represents three experiments exhibiting similar results.

loading controls (Fig. 2*A, a* and *b, bottom*). The results indicated that osteopontin enhanced PKCα phosphorylation and its interaction with c-Src. To determine the role of $\alpha_v\beta_3$ integrin on osteopontin-induced PKCα phosphorylation, cells were pretreated with anti-human $\alpha_v\beta_3$ integrin blocking antibody, RGD, or RGE (GpenGRGDSPCA and GRGESP, respectively) peptides and then treated with osteopontin, and the level of PKCα phosphorylation was detected by immunoblotting. The results indicated that anti-$\alpha_v\beta_3$ integrin blocking antibody and GpenGRGDSPCA but not GRGESP suppressed the osteopontin-induced PKCα phosphorylation (data not shown). The data suggested that $\alpha_v\beta_3$ integrin plays an important role in osteopontin-induced PKCα phosphorylation. To delineate whether PKCα is upstream of c-Src or vice versa, cells were pretreated with PKCα inhibitor (staurosporine) and treated with osteopontin, and cell lysates were immunoprecipitated with anti-c-Src antibody. The immunoprecipitated samples were analyzed for c-Src autophosphorylation by *in vitro* kinase assay. Similarly, in other experiments, cells were transfected with dn c-Src and treated with osteopontin, and cell lysates were immunoprecipitated with anti-PKCα. The immunoprecipitated samples were used for *in vitro* PKCα kinase assay. The data showed that dn c-Src has no effect on PKCα autophosphorylation, whereas PKCα inhibitor suppressed c-Src phosphorylation, suggesting that osteopontin regulates PKCα-dependent c-Src activation (Fig. 2*B, a* and *b, top*). The levels of PKCα and c-Src in the same lysates were detected by Western blot using their specific antibodies as controls (Fig. 2*B, a* and *b, bottom*). Furthermore, suppression of PKCα and c-Src resulted in inhibition of osteopontin-induced NIK phosphorylation (data not shown). To determine whether these upstream kinases (PKC, c-Src, and NIK) play any role in osteopontin-induced IKKα/β phosphorylation, cells were individually transfected with dn c-Src or wt and mut NIK or pretreated with PKCα inhibitor (staurosporine) and then treated with osteopontin. Cell lysates were analyzed either by Western blot using anti-phosphoserine IKKα/β antibody or immunoprecipitated with anti-IKKα/β antibody followed by immunoblotting with anti-phosphotyrosine antibody (Fig. 2*C, top* and *middle*). These data showed that both PKC inhibitor and dn c-Src suppressed osteopontin-induced serine and tyrosine phosphorylations of IKKα/β, whereas mut NIK inhibits only the serine but not tyrosine phosprylation of IKKα/β, suggesting that NIK plays differential role in osteopontin-induced PKCα/c-Src–mediated IKKα/β activation (Fig. 2*C, top* and *middle*). The level of IKK α/β was also detected by Western blot as control (Fig. 2*C, bottom*).

To further investigate whether PKCα, c-Src, NIK, IKK, and NF-κB play any role in osteopontin-induced COX-2 expression, cells were pretreated with PKC inhibitor (staurosporine) or individually transfected with dn c-Src, wt and mut NIK, and IκBα super-repressor, wt and dn IKKα or IKKβ followed by treatment with osteopontin. The COX-2 expression was detected by Western blot (Fig. 2*D*). These results suggested that PKCα and c-Src play an important role in regulating osteopontin-induced COX-2 expression through a NIK/IKK/NF-κB–mediated pathway.

Osteopontin induces PKCα/c-Src–mediated p65 phosphorylation. Recent findings suggested that phosphorylation of p65 subunit of NF-κB leads to nuclear translocation and activation of NF-κB (35), and that the promoter region of COX-2 contains the NF-κB response element (36). In Fig. 2*D*, we showed that suppression of NF-κB by overexpression of IκBα super-repressor significantly inhibits osteopontin-induced COX-2 expression. Therefore, we sought to determine whether osteopontin regulates NF-κB, p65 phosphorylation that ultimately regulates COX-2 expression, and whether PKCα and c-Src are involved in this process. Accordingly, cells were treated with osteopontin from 0 to 180 minutes or pretreated with PKC inhibitor (staurosporine) or transfected with dn c-Src and then treated with osteopontin. The level of p65 phosphorylation in the cell lysates was detected by

Western blot using anti-phospho-p65 antibody (Fig. 3*A* and *B*). The results showed that inhibition of PKCα and c-Src significantly suppressed osteopontin-induced NF-κB, p65 phosphorylation (Fig. 3*B*). These results clearly suggested that osteopontin induces p65 phosphorylation through a PKCα/c-Src–dependent pathway, which leads to NF-κB activation that ultimately regulates COX-2 expression.

Osteopontin augments COX-2-mediated PGE_2 production and MMP-2 activation. Earlier reports revealed that overexpression of COX-2 leads to up-regulation of arachidonic acid metabolism, which in turn results in enhancement of PGE_2 production and tumor progression (2, 37–39). Accordingly, to determine whether osteopontin can induce COX-2-mediated PGE_2 production, cells were treated with osteopontin for 0 to 24 hours, and the PGE_2 level in the conditioned media was measured by using PGE_2 enzyme immunoassay kit. To examine whether PKC, c-Src, and COX-2 are involved in osteopontin-induced PGE_2 production, cells were pretreated with PKC inhibitor (staurosporine) or COX-2 inhibitor (celecoxib) or transfected with dn c-Src and then treated with osteopontin. The results indicated that inhibitors of PKC and COX-2 and dn c-Src drastically suppressed the osteopontin-induced PGE_2 production (Fig. 3*D* and *E*). To delineate the role of PKCα, c-Src, and COX-2 in osteopontin-induced MMP-2 activation, cells were treated or transfected as described earlier, and the level of active MMP-2 in the conditioned medium was determined by zymography (Fig. 3*C*). These results showed that COX-2 plays a crucial role in osteopontin-induced PKC/c-Src–mediated PGE_2 production and MMP-2 activation in prostate cancer cells.

COX-2 and PGE_2 play an important role in osteopontin-induced PC-3 cell migration and invasion. Previous data suggested that COX-2 and its metabolite PGE_2 act as crucial molecules in regulating tumor cell motility, invasiveness, and tumor metastasis (2). Therefore, to examine the role of COX-2 and PGE_2 in osteopontin-mediated PC-3 cell migration, the wound assay was done. Cells were either pretreated with PKC inhibitor (staurosporine), celecoxib, or anti-EP2 antibody or transfected with dn c-Src. Wounds with a constant diameter were made, and cells were treated with osteopontin. The wound photographs were taken under phase-contrast microscope (Fig. 4*A*). These data showed that inhibition of COX-2 or its upstream kinases (PKCα and c-Src) resulted in significant suppression of osteopontin-induced PC-3 cell motility towards the wound and further indicated that COX-2 act as a key molecule in osteopontin-induced tumor cell migration. Interestingly, blocking the interaction between PGE_2 and its receptor EP2 by using specific anti-EP2 blocking antibody also suppressed osteopontin-induced tumor cell motility, indicating that osteopontin regulates wound migration via COX-2-dependent PGE_2 production through interaction with its receptor EP2 in an autocrine fashion. The wound migration data were further confirmed by modified Boyden chamber migration and extracellular matrix invasion assays. The results indicated that the cell migration due to over expression of wt NIK, IKKα, or IKKβ in response to osteopontin was suppressed by the celecoxib, suggesting the potential role of COX-2 in osteopontin-induced NIK/IKK–dependent tumor cell migration and invasion (Fig. 4*B* and *C*). To examine the specificity of COX-2 in osteopontin-induced cell migration, NS398 (NSAID), a COX-2 inhibitor, was used, and the data showed that NS398 is also suppressed osteopontin-induced cell migration and invasion. PGE_2 was used as a positive control. Taken together, these data indicated the potential and crucial role of COX-2 and PGE_2 in osteopontin-induced tumor cell motility and invasiveness.

Osteopontin-induced tumor cell–derived PGE_2 enhanced endothelial cell motility and invasiveness through paracrine mechanism. Earlier data indicated that tumor-derived PGE_2

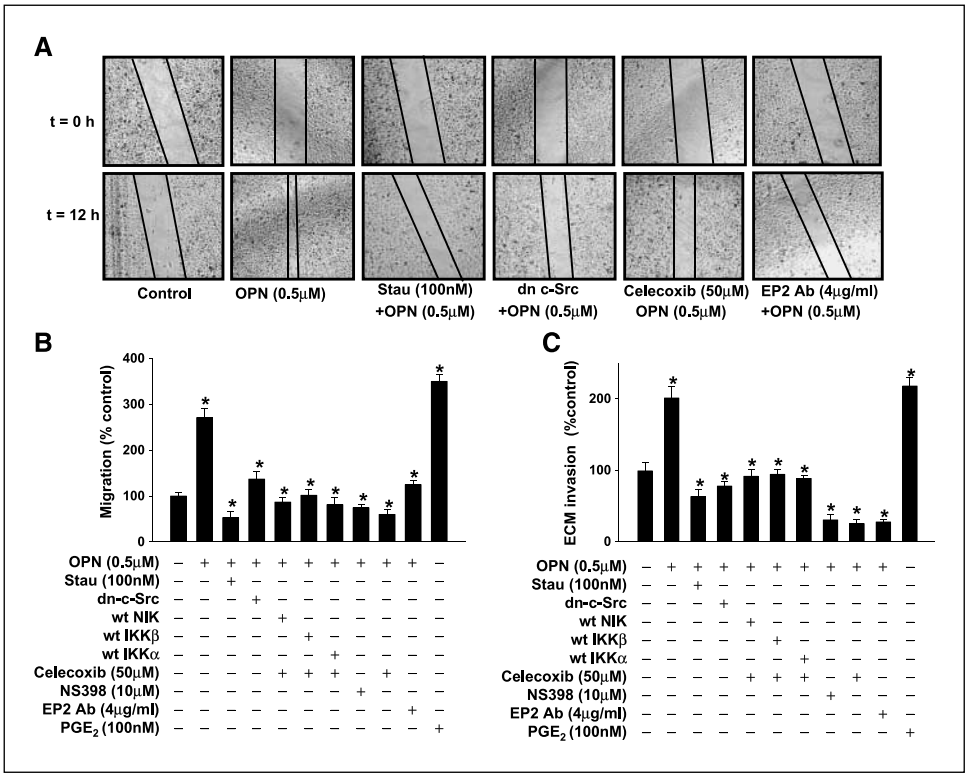

Figure 4. Inhibition of the PKC, c-Src, and COX-2 or blocking of EP2 receptor suppressed osteopontin (*OPN*)–induced PC-3 cell motility and invasiveness. *A,* cells were transfected with dn c-Src, or pretreated with staurosporine (*Stau*), celecoxib, or anti-EP2 blocking antibody (4 μg) then treated with osteopontin for 12 hours. Wound assays were done as described earlier. Wound photographs were taken at initial time (0 hour) and the termination of the experiments (12 hours). The experiments were repeated in triplicate. *B,* cells were individually transfected with wt NIK and IKKα and IKKβ and treated with celecoxib. In separate experiments, cells were transfected with dn c-Src or treated with staurosporine, celecoxib, NS398, and EP2 blocking antibody and used for migration assay. Osteopontin was used in the upper chamber. PGE_2 was used as positive control. After 12 hours, migrated cells were counted from the lower chamber and represented graphically. *C,* experiments paralleling those of (*B*) but measuring invasion rather than migration. *Columns,* means of three determinations; *bars,* SE.

interacts with the endothelial cell surface receptor and induced endothelial cell motility and invasiveness that leads to tumor angiogenesis (38). It is reported that EP2 act as one of the main PGE_2 receptor in endothelial cells (39). To determine whether osteopontin-induced PC-3 cell–derived PGE_2 enhances endothelial cell migration and invasion through EP2-mediated paracrine manner, endothelial cells were used on the upper side of modified Boyden or Matrigel-coated invasion chamber. The conditioned media collected from osteopontin-treated PC-3 cells were used as chemoattractrant (Fig. 5*A* and *B*). In separate experiments, endothelial cells were pretreated with anti-EP2 blocking antibody and used for migration and invasion assays. Our data showed that conditioned media of osteopontin-treated PC-3 cells significantly enhanced endothelial cell migration and invasion, whereas blocking the EP2 receptor in these cells with its antibody significantly suppressed the endothelial cell migration and invasion (Fig. 5*A* and *B*). The enhanced migration of endothelial cells was further confirmed by wound assay under the same experimental condition (Fig. 5*C*). Our results indicated that osteopontin-induced tumor cell–derived PGE_2 enhanced migration and invasion of endothelial cells through an EP2-mediated paracrine mechanism.

Development of PC-3 xenograft model to study the role of COX-2 in osteopontin-induced tumor progression. Our *in vitro* results prompted us to study the role of COX-2 and PGE_2 in osteopontin-induced mice xenograft tumor progression. Accordingly, PC-3 cells (5×10^5) were mixed with Matrigel and then injected s.c. into the dorsal flanks of the male athymic nude mice. In other experiments, cells were treated with osteopontin alone or along with anti-EP2 blocking antibody and then injected into the nude mice. The osteopontin alone or mixture of osteopontin and anti-EP2 antibody was also injected to the tumor sites twice a week for up to 4 weeks. In another experiments, celecoxib (1,500 ppm) was supplemented to the normal diet of the osteopontin-injected animals. All the mice were kept under pathogen-free conditions. Figure 6*A* (*a-d*) showed typical photographs of tumors grown in nude mice. Blood was collected; mice were sacrificed by cervical dislocation; and tumors were excised, weighed, and measured (Table 1). Tumor samples were used for histopathologic and immunohistochemical studies according to standard procedure. The histopathologic analysis by H&E staining is summarized in Table 2, and these data clearly indicated that osteopontin-induced tumorigenicity in nude mice was suppressed significantly by anti-EP2 blocking antibody or by supplementation of celecoxib in mice diet (Table 2; Fig. 6*A, e-h*). Moreover, the immunohistochemical studies showed that the enhanced expressions of COX-2 and MMP-2 were detected in mice treated with osteopontin (Fig. 6*A, i-p*). The expression of vWF (an endothelial cell–specific marker) was also detected (Fig. 6*A, q-t*). The plasma PGE_2 level was also higher in osteopontin injected mice (Fig. 6*B*). Taken together, our *in vivo* xenograft study showed that osteopontin induces prostate tumor growth and angiogenesis in nude mice that is correlated with up-regulation of COX-2 expression, MMP-2 activation, and PGE_2 secretion. Inhibition of COX-2 or blocking of EP2 receptor significantly suppressed osteopontin-induced angiogenesis and tumor progression in nude mice and further showed that COX-2 plays an important role in osteopontin-induced prostate cancer progression.

Expressions of osteopontin, COX-2, MMP-2, and NF-κB, p65 localization, and their correlation with human prostate cancer progression and angiogenesis in different pathologic grades. To correlate the *in vitro* data and *in vivo* mouse model results with human clinical specimens, human prostate cancer tissues were collected from a local hospital with informed consent. The tumor samples were stained with H&E, and the grades of these samples were determined by Gleason grading system with the help of expert histoplathologist (Fig. 7*A, a-c*). Expression of osteopontin, COX-2, MMP-2, and vWF and cellular localization of p65 were analyzed by immunohistochemistry using their specific

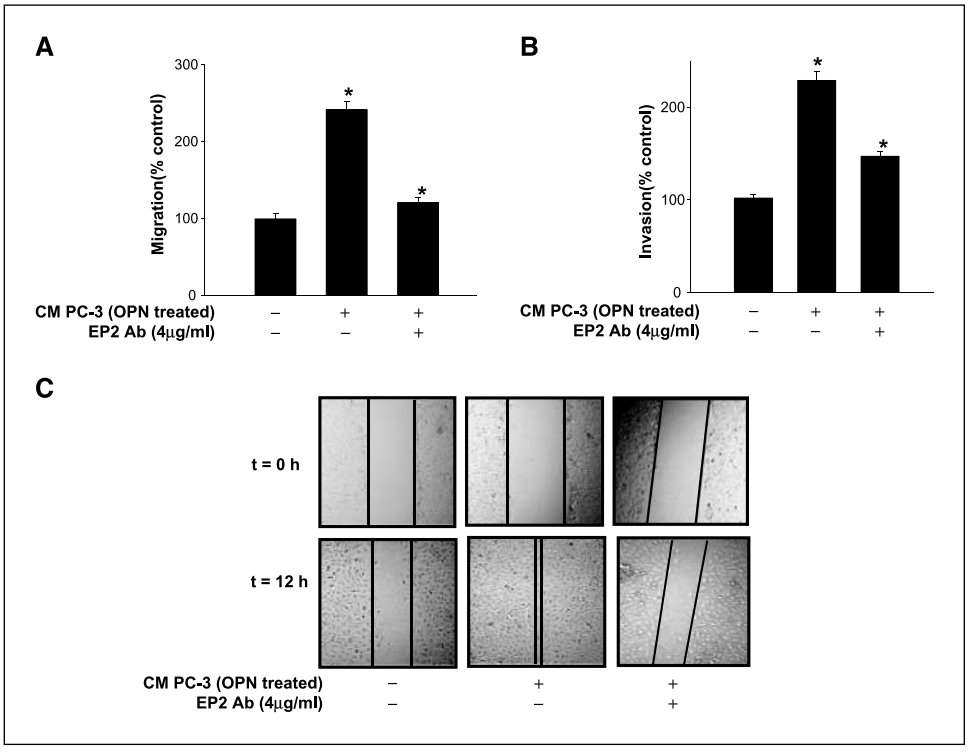

Figure 5. Osteopontin (*OPN*) stimulates EP2-mediated endothelial cell migration, invasion, and wound healing via paracrine mechanism. *A,* human endothelial (EA.hy-926) cells were added in the upper chamber. The conditioned medium (*CM*) collected from PC-3 cells treated with osteopontin was used as chemoattractant in the lower chamber. In separate experiments, EA.hy-926 cells were treated with anti-EP2 blocking antibody and used for migration assay. After 12 hours, migrated cells were counted as described earlier. *B* and *C,* experiments paralleling those of (*A*) but measuring invasion and wound healing rather than migration. *Columns,* means of three determinations; *bars,* SE.

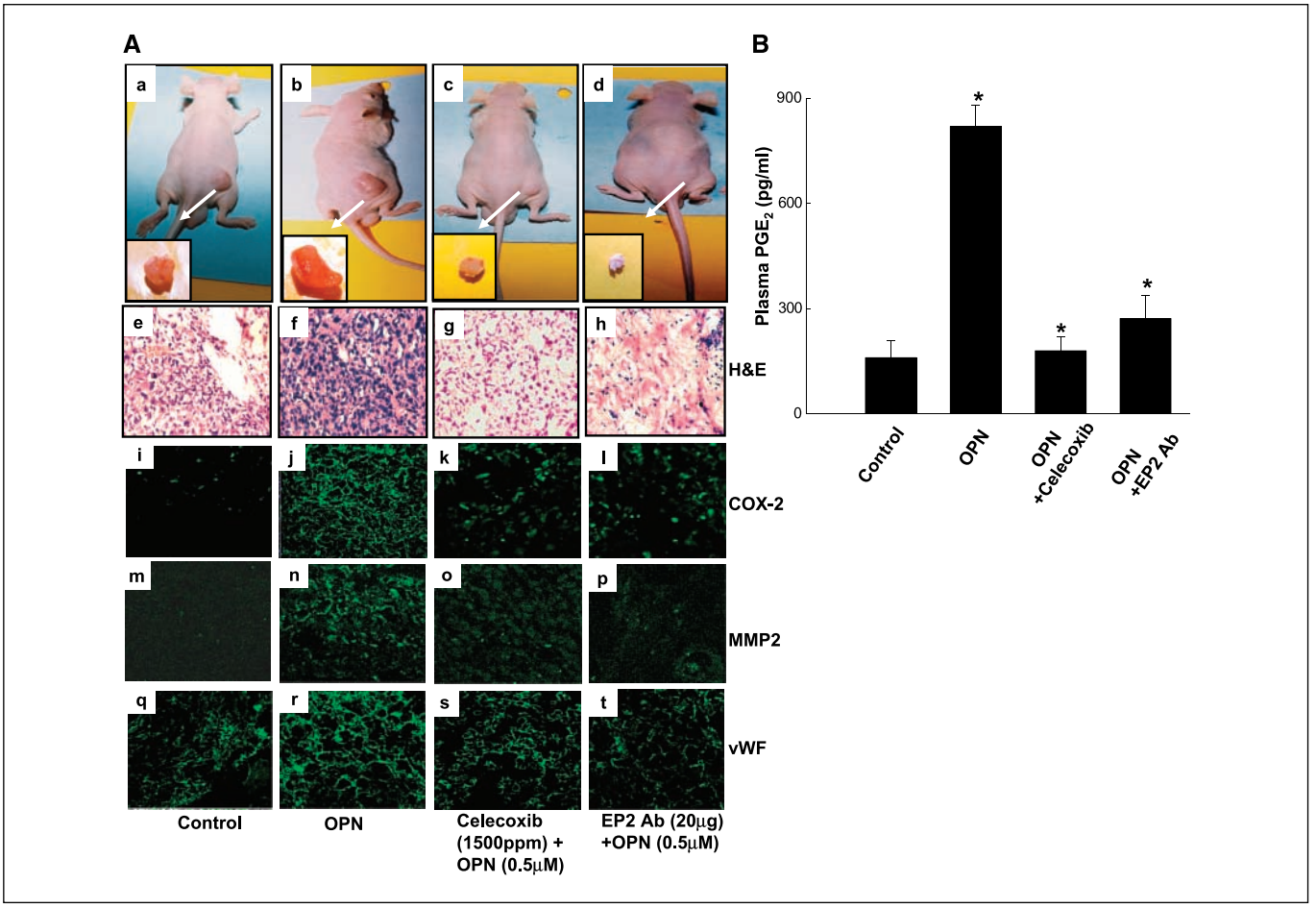

Figure 6. COX-2 and PGE_2 play crucial roles in osteopontin (*OPN*)–induced tumorigenesis and angiogenesis in nude mice. *A,* photographs of athymic mice showing 4-week-old xenograft tumor growth by PC-3 cells; *inset,* excised tumors with respective mice (*a-d*). Experimental details were described in Materials and Methods. Representative H&E-stained sections from PC-3 xenograft tumors and the characteristics of these tumors were analyzed (*e-h*). The expression of COX-2 (*i-l*), MMP-2 (*m-p*), and neovascularization (vWF expression; *q-t*) were visualized by immunofluorescence study using their specific antibodies. COX-2, MMP-2, and vWF were stained with FITC-conjugated IgG (*green*). *B,* levels of PGE_2 production in these mice were determined from mice plasma by enzyme immunoassay. Three mice were used in each set of experiments.

antibodies (Fig. 7*A, d-r*). These results indicated the higher levels of osteopontin and COX-2 in malignant tumors than normal and PIN, and that further correlated with the enhanced MMP-2 expression and neovascularization (vWF expression). Moreover, there was significant nuclear translocation of p65 in the malignant tumors. All these data correlate with our *in vitro* and mice xenograft studies.

Discussion

The interaction between osteopontin and prostate cancer cells are likely to be the key determinants in regulating tumor progression and metastatic phenotype of human prostate carcinoma and further indicates that osteopontin may be an important mediator of prostate cancer progression (40). Recent strategies in therapeutics of prostate cancers with inhibitors that target COX-2 (41) and its enhanced expression in prostate carcinoma suggest that understanding the molecular mechanism underlying enhanced COX-2 expression may help in developing the novel therapeutic approach in prostate cancer treatment. The experimental work presented in the study showed for the first time the molecular mechanism that underlies osteopontin-induced COX-2 expression and its potential role in regulating *in vitro* cell motility and invasion of prostate cancer, which ultimately modulates *in vivo* tumor growth and angiogenesis. Silencing of osteopontin in prostate cancer cells results drastic reduction, whereas overexpression of osteopontin significantly increased COX-2 level, suggesting the specificity of osteopontin on COX-2 expression. Moreover, we find that COX-2 plays an important role in osteopontin-induced PGE_2 production and MMP-2 activation that ultimately regulates tumor progression.

Table 1. Effect of COX-2 inhibition and EP2 receptor blocking on osteopontin-induced prostate tumor growth in nude mice

No. mice	Treatments	Tumor wt (fold changes)
3	Control	1.00 ± 0.13
3	Osteopontin	2.83 ± 0.17
3	Osteopontin + celecoxib (1,500 ppm)	0.52 ± 0.14
3	Osteopontin + EP2 antibody (20 μg)	0.12 ± 0.10

Table 2. Characteristics of the xenograft tumors from experimental mice

Tumor characteristics	Control	Osteopontin (0.5 μmol/L)	Osteopontin (0.5 μmol/L) + celecoxib (1,500 ppm)	Osteopontin (0.5 μmol/L) + EP2 antibody (20 μg)
Tumor infiltration	Moderate	Very high	Moderate to poor	Poor
Vessel formation	Poor	High	Moderate to poor	Negligible
Mitotic features/hpf	4-6	12-16	2-4	1-3
Tumor giant cells	Less	Plenty	Scanty	Very less
Nuclear polymorphism	Moderate nuclear size variation	Marked nuclear size variation	Less nuclear size variation	Small regular uniform nucleus

In prostate cancer, PKCα plays a key role in the regulation of downstream oncogenic molecules (34). Recent reports also revealed that activation of PKCα is required for the survival and growth of androgen-independent human prostate cancer cells (41–43). However, it is not well established how osteopontin regulates PKCα activation and PKCα-dependent downstream signaling events in prostrate carcinoma. In this study, we provide evidences that PKCα plays an important role in osteopontin-induced c-Src/NIK–mediated IKKα/β-dependent NF-κB phosphorylation, which ultimately controls COX-2 expression. Recently, we have shown the involvement of the NIK/IKK/NF-κB signaling pathway in osteopontin-induced expression of downstream effecter molecules that regulate melanoma and breast tumor progression (21, 27). In this study, we report that osteopontin regulates PKCα/c-Src–mediated

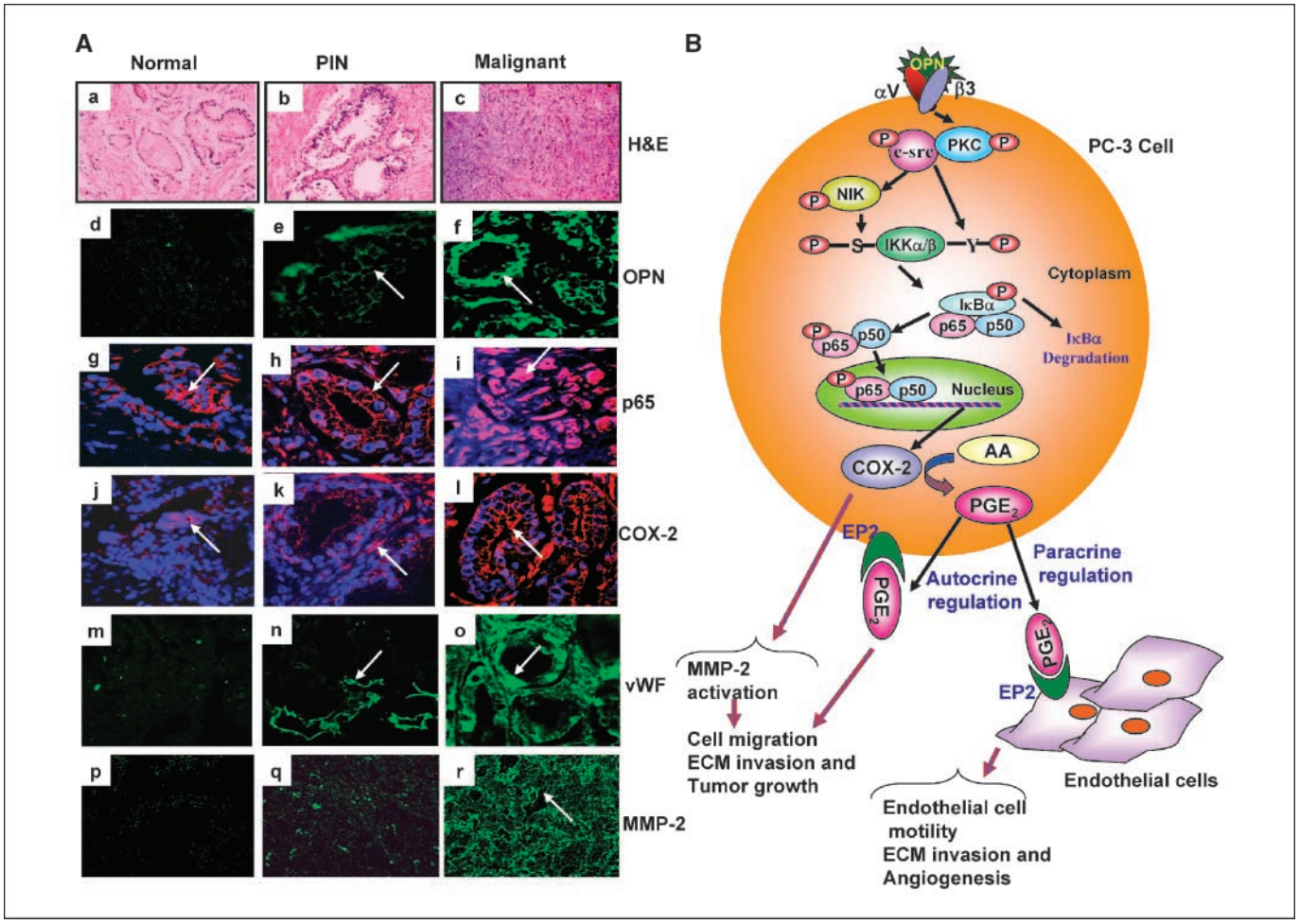

Figure 7. Expressions of osteopontin (*OPN*), COX-2, MMP-2, and NF-κB; p65 localization; and their correlation with human prostate cancer progression and angiogenesis in different pathological grades. *A,* prostate tumor specimens were collected from a local hospital with informed consent. The gradations of these specimens were done according to the Gleason grading system by H&E staining (*a-c*). The levels of osteopontin (*d-f*), COX-2 (*j-l*), vWF (*m-o*), and MMP-2 (*p-r*) expression and cellular localization of p65 (*g-i*) were detected by immunohistochemical studies using their specific antibodies. Osteopontin, vWF, and MMP-2 were stained with FITC (*green*), whereas COX-2 and p65 (NF-κB) were stained with TRITC (red)–conjugated IgG, and the nucleus was counterstained with 4′,6-diamidino-2-phenylindole (*blue*). *B,* schematic representation of osteopontin-induced PKCα/c-Src/IKK/NF-κB–mediated COX-2 expression leading to enhanced PGE_2 production and MMP-2 activation that further induces tumorigenesis and angiogenesis via autocrine and paracrine mechanisms.

IKK activation followed by NF-κB phosphorylation. Moreover, the results showed that overexpression of super-repressor form of IκBα significantly suppressed osteopontin-induced COX-2 expression, suggesting that NF-κB act as the key transcription factor in regulation of COX-2 expression and further showed the dispensability of the PKCα/c-Src/IKK/NF-κB signaling cascade in osteopontin-induced COX-2 expression.

It is well established that increased level of PGE_2 production and MMP-2 activation is associated with enhanced expression of COX-2 in many cancers (44, 45). Administration of COX-2 inhibitors has been reported to suppress PGE_2 production and MMP-2 activation in various cancers (46–48). Recent reports also indicated that PGE_2 could also induce MMP-2 activation in cancer cells (49). Our data showed that inhibition of upstream signaling pathway or treatment with COX-2 inhibitor (celecoxib) significantly suppressed osteopontin-induced PGE_2 production and MMP-2 activation.

Recent findings indicated that COX-2-specific inhibitors significantly suppressed tumor growth in prostate cancer (50). Interestingly, our studies showed that NSAID celecoxib and NS398 (COX-2-selective inhibitor) significantly suppressed osteopontin-induced PC-3 cells migration and invasion. The *in vivo* xenograft tumor experiment indicated that mice fed with celecoxib showed significant reduction in osteopontin-induced tumor growth, and this study suggested that COX-2 could be an effective target in caner therapy.

Tumor cell–derived PGE_2 can contribute tumor progression by regulating the cell motility/invasiveness and inducing angiogenesis (8–10). Among PGE_2 receptors, EP2 is expressed in both prostate cancer and endothelial cells (39, 51). Moreover, the development of selective antagonists against the EP2 receptor has the potential to improve antitumor activity, and EP2 receptor antagonist may be more specific than the use of COX-2 inhibitors (52). Sung et al. showed that tumors from wt EP2 mice produced more blood vessels than those of knockout mice (53). In our study, we showed that the blocking the EP2 receptor by specific blocking antibody suppressed osteopontin-induced prostate cancer (PC-3) and endothelial cell motility and invasiveness. Furthermore, we also find that administration of anti-EP2 blocking antibody significantly suppressed osteopontin-induced mice xenograft tumor progression.

Our study showed the detailed molecular mechanism by which osteopontin induces cell migration, invasion, and tumor progression through induction of COX-2 expression and PGE_2 production (Fig. 7*B*). Our results further warrant that the mechanism shown in the mouse model underlies the human pathology and a clear understanding of osteopontin and COX-2 regulation could illuminate cellular changes that accompany prostate cancer progression and may facilitate the development of novel therapeutic approaches to suppress osteopontin-regulated PKCα/IKK/NF-κB–mediated COX-2 expression and thereby controlling tumor progression and angiogenesis.

Acknowledgments

Received 2/20/2006; accepted 5/2/2006.

Grant support: National Bioscience Award Fund for Career Development (G.C. Kundu); Department of Biotechnology, Government of India; and Council of Scientific and Industrial Research, Government of India (S. Jain).

The costs of publication of this article were defrayed in part by the payment of page charges. This article must therefore be hereby marked *advertisement* in accordance with 18 U.S.C. Section 1734 solely to indicate this fact.

We thank Dr. Ajay Gangshettiwar for histopathologic studies.

References

1. McCarty MF. Targeting multiple signaling pathways as a strategy for managing prostate cancer: multifocal signal modulation therapy. Integr Cancer Ther 2004;3:349–80.
2. Wallace JM. Nutritional and botanical modulation of the inflammatory cascade—eicosanoids, cyclooxygenases, and lipoxygenases—as an adjunct in cancer therapy. Integr Cancer Ther 2002;1:7–37.
3. DeWitt D, Smith WL. Yes, but do they still get headaches? Biochem Cell 1995;83:345–8.
4. DeWitt DL. Prostaglandin endoperoxide synthase: regulation of enzyme expression. Biochim Biophys Acta 1991;1083:121–34.
5. Smith WL, Meade EA, DeWitt DL. Pharmacology of prostaglandin endoperoxide synthase isozymes-1 and -2. Ann N Y Acad Sci 1994;714:136–42.
6. Chandrasekharan NV, Dai H, Roos KL, et al. COX-3, a cyclooxygenase-1 variant inhibited by acetaminophen and other analgesic/antipyretic drugs: cloning, structure, and expression. Proc Natl Acad Sci U S A 2002;99:13926–31.
7. Chaudry AA, Wahle KW, McClinton S, Moffat LE. Arachidonic acid metabolism in benign and malignant prostatic tissue *in vitro*: effects of fatty acids and cyclooxygenase inhibitors. Int J Cancer 1994;57:176–80.
8. Wang D, DuBois RN. Cyclooxygenase 2-derived prostaglandin E2 regulates the angiogenic switch. Proc Natl Acad Sci U S A 2004;101:415–6.
9. Houchen CW, Sturmoski MA, Anant S, Breyer RM, Stenson WF. Prosurvival and antiapoptotic effects of PGE_2 in radiation injury are mediated by EP2 receptor in intestine. Am J Physiol Gastrointest Liver Physiol 2003;284:490–8.
10. Gately S, Li WW. Multiple roles of COX-2 in tumor angiogenesis: a target for antiangiogenic therapy. Semin Oncol 2004;31:2–11.
11. Sales KJ, Katz AA, Davis M, et al. Cyclooxygenase-2 expression and prostaglandin E (2) synthesis are upregulated in carcinomas of the cervix: a possible autocrine/paracrine regulation of neoplastic cell function via EP2/EP4 receptors. J Clin Endocrinol Metab 2001;86:2243–9.
12. Rangaswami H, Bulbule A, Kundu GC. Osteopontin: role in cell signaling and cancer progression. Trends Cell Biol 2006;16:79–87.
13. Rittling SR, Chambers AF. Role of osteopontin in tumor progression. Br J Cancer 2004;90:1877–81.
14. Denhardt DT, Guo X. Osteopontin: a protein with diverse functions. FASEB J 1993;7:1475–82.
15. Weber GF, Ashkar S, Glimcher MJ, Cantor H. Receptor-ligand interaction between CD44 and osteopontin (Eta-1). Science 1996;271:509–12.
16. Panda D, Kundu GC, Lee BI, et al. Potential roles of osteopontin and alphaVbeta3 integrin in the development of coronary artery restenosis after angioplasty. Proc Natl Acad Sci U S A 1997;94:9308–13.
17. Liaw L, Birk DE, Ballas CB, Whitsitt JS, Davidson JM, Hogan BL. Altered wound healing in mice lacking a functional osteopontin gene (spp1). J Clin Invest 1998;101:1468–78.
18. Sodek J, Ganss B, McKee MD. Osteopontin. Crit Rev Oral Biol Med 2000;11:279–303.
19. Angelucci A, Festuccia C, D'Andrea G, Teti A, Bologna M. Osteopontin modulates prostate carcinoma invasive capacity through RGD-dependent upregulation of plasminogen activators. Biol Chem 2002;383:229–34.
20. Philip S, Bulbule A, Kundu GC. Osteopontin stimulates tumor growth and activation of promatrix metalloproteinase-2 through nuclear factor-kappa B-mediated induction of membrane type 1 matrix metalloproteinase in murine melanoma cells. J Biol Chem 2001;276:44926–35.
21. Das R, Mahabeleshwar GH, Kundu GC. Osteopontin stimulates cell motility and nuclear factor kappa B-mediated secretion of urokinase type plasminogen activator through phosphatidylinositol 3-kinase/Akt signaling pathways in breast cancer cells. J Biol Chem 2003;278:28593–606.
22. Aprikian AG, Tremblay L, Han K, Chevalier S. Bombesin stimulates the motility of human prostate-carcinoma cells through tyrosine phosphorylation of focal adhesion kinase and of integrin-associated proteins. Int J Cancer 1997;72:498–504.
23. Huang WC, Chen JJ, Inoue H, Chen CC. Tyrosine phosphorylation of I-kappa B kinase alpha/beta by protein kinase C-dependent c-Src activation is involved in TNF-alpha-induced cyclooxygenase-2 expression. J Immunol 2003;170:4767–75.
24. Rodrigues S, Nguyen QD, Faivre S, et al. Activation of cellular invasion by trefoil peptides and src is mediated by cyclooxygenase- and thromboxane A2 receptor-dependent signaling pathways. FASEB J 2001;15:1517–28.
25. Baeuerle PA, Baltimore D. NF-kappa B: ten years after. Cell 1996;87:13–20.
26. Malinin NL, Boldin MP, Kovalenko AV, Wallach D. MAP3K-related kinase involved in NF-kappaB induction by TNF, CD95 and IL-1. Nature 1997;385:540–4.
27. Rangaswami H, Bulbule A, Kundu GC. Nuclear factor-inducing kinase plays a crucial role in osteopontin-induced MAPK/IkappaBalpha kinase-dependent nuclear factor kappaB-mediated promatrix metalloproteinase-9 activation. J Biol Chem 2004;279:38921–35.
28. Inoue H, Yokoyama C, Hara S, Tone Y, Tanabe T. Transcriptional regulation of human prostaglandin endoperoxide synthase-2 gene by lipopolysaccharide and phorbol esters in vascular endothelial cells.

Involvement of both nuclear factor for interleukin-6 expression site and cAMP response element. J Biol Chem 1995;270:24965–71.
29. Inaba T, Sano H, Kawahito Y, et al. Induction of cyclooxygenase-2 in monocyte/macrophage by mucins secreted from colon cancer cells. Proc Natl Acad Sci U S A 2003;100:2736–41.
30. Zhang P, Ostrander JH, Faivre EJ, Olsen A, Fitzsimmons D, Lange CA. Regulated association of protein kinase B/Akt with breast tumor kinase. J Biol Chem 2005;280:1982–91.
31. Leopold JA, Walker J, Scribner AW, et al. Glucose-6-phosphate dehydrogenase modulates vascular endothelial growth factor-mediated angiogenesis. J Biol Chem 2003;278:32100–6.
32. Zweifel BS, Davis TW, Ornberg RL, Masferrer JL. Direct evidence for a role of cyclooxygenase-2-derived prostaglandin E2 in human head and neck xenograft tumors. Cancer Res 2002;62:6706–11.
33. Chakraborty G, Rangaswami H, Jain S, Kundu GC. Hypoxia regulates crosstalk between Syk and Lck leading to breast cancer progression and angiogenesis. J Biol Chem 2006;281:11322–31.
34. Stewart JR, O'Brian CA. Protein Kinase C-alpha mediates epidermal growth factor receptor transactivation in human prostate cancer cells. Mol Cancer Ther 2005;4:726–32.
35. Ghosh S, Karin M. Missing pieces in the NF-kappa B puzzle. Cell 2002;109:S81–96.
36. Kosaka T, Miyata A, Ihara H, et al. Characterization of the human gene (PTGS2) encoding prostaglandin-endoperoxide synthase 2. Eur J Biochem 1994; 221:889–97.
37. Timoshenko AV, Xu G, Chakrabarti S, Lala PK, Chakraborty C. Role of prostaglandin E 2 receptors in migration of murine and human breast cancer cells. Exp Cell Res 2003;289:265–74.
38. Salcedo R, Zhang X, Young HA, et al. Angiogenic effects of PGE 2 are mediated by up-regulation of CXCR4 on human microvascular endothelial cells. Blood 2003;102:1966–77.
39. Cattaneo MG, Pola S, Deho V, Sanguini AM, Vicentini LM. Alprostadil suppresses angiogenesis *in vitro* and *in vivo* in the murine matrigel plug assay. Br J Pharmacol 2003;138:377–85.
40. Thalmann GN, Sikes RA, Devoll RE, et al. Osteopontin: possible role in prostate cancer progression. Clin Cancer Res 1999;5:2271–7.
41. Karamouzis MV, Papavassiliou AG. COX-2 inhibition in cancer therapeutics: a field of controversy or a magic bullet? Expert Opin Investig Drugs 2004;13: 359–72.
42. Koren R, Ben Meir D, Langzam L, et al. Expression of protein kinase C isoenzymes in benign hyperplasia and carcinoma of prostate. Oncol Rep 2004;11:321–6.
43. O'Brian CA. Protein kinase C-alpha: a novel target for the therapy of androgen-independent prostate cancer? Oncol Rep 1998;5:305–9.
44. Mayoral R, Fernandez-Martinez A, Bosca L, Martin-Sanz P. Prostaglandin E2 promotes migration and adhesion in hepatocellular carcinoma cells. Carcinogenesis 2005;26:753–61.
45. Dohadwala M, Batra RK, Luo J, et al. Autocrine/paracrine prostaglandin E2 production by non-small cell lung cancer cells regulates matrix metalloproteinase-2 and CD44 in cyclooxygenase-2-dependent invasion. J Biol Chem 2002;277:50828–33.
46. Pan MR, Chuang LY, Hung WC. Non-steroidal anti-inflammatory drugs inhibit matrix metalloproteinase-2 expression via repression of transcription in lung cancer cells. FEBS Lett 2001;508:365–8.
47. Nagatsuka I, Yamada N, Shimizu S, et al. Inhibitory effect of a selective cyclooxygenase-2 inhibitor on liver metastasis of colon cancer. Int J Cancer 2002; 100:515–9.
48. Attiga FA, Fernandez PM, Weeraratna AT, Manyak MJ, Patierno SR. Inhibitors of prostaglandin synthesis inhibit human prostate tumor cell invasiveness and reduce the release of matrix metalloproteinases. Cancer Res 2000;60:4629–37.
49. Ito H, Duxbury M, Benoit E, et al. Prostaglandin E_2 enhances pancreatic cancer invasiveness through an Ets-1-dependent induction of matrix metalloproteinase-2. Cancer Res 2004;64:7439–46.
50. Gupta S, Adhami VM, Subbarayan M, et al. Suppression of prostate carcinogenesis by dietary supplementation of celecoxib in transgenic adenocarcinoma of the mouse prostate model. Cancer Res 2004;64: 3334–43.
51. Chen Y, Hughes-Fulford M. Prostaglandin E2 and the protein kinase A pathway mediate arachidonic acid induction of c-fos in human prostate cancer cells. Br J Cancer 2000;82:2000–6.
52. Pavlovic S, Du B, Sakamoto K, et al. Targeting PGE 2 receptors as an alternative strategy to block COX-2-dependent extracellular matrix-induced MMP-9 expression by macrophages. J Biol Chem 2006;281:3321–8.
53. Sung YM, He G, Fischer SM. Lack of expression of the EP2 but not EP3 receptor for prostaglandin E2 results in suppression of skin tumor development. Cancer Res 2005;65:9304–11.